Proceedings of ASME Turbo Expo 2023
Turbomachinery Technical Conference and Exposition
GT2023
June 26-30, 2023, Boston, Massachusetts

GT2023-102402

ENERGY MANAGEMENT SYSTEM FOR SMART GRIDS INCLUDING RENEWABLE SOURCES AND INDUSTRIAL SYMBIOSIS

Mario L. Ferrari mario.ferrari@unige.it
Lorenzo Gini lorenzo.gini@edu.unige.it
Simone Maccarini simone.maccarini@edu.unige.it

University of Genoa
Genova, Italy

ABSTRACT

The aim of this work regards the development of an energy management system (EMS) for smart grids with a high integration level of renewable sources. Special attention is devoted to waste recycling due to a large industrial symbiosis involving the production of alternative fuels (syngas and biogas). In details, the paper focuses attention on the Eigerøy island (Norway) that will be the demonstration site of the ongoing EU ROBINSON project. The main purpose of this activity is the development of technology integration solutions for decarbonization path, starting from industrialized districts in islands and considering high flexibility for replication issues.

The mentioned technology integration is obtained with an EMS able to operate in real-time mode for minimization of energy costs (fuels and electricity). So, this tool includes a minimization subroutine for calculating the optimal operative condition (on/off status for generators and the related set-points) connected with a Model Predictive Control (MPC) software for the real-time calculation of the generator set-points. An innovative approach is the integration of the electrolyzer management scheduling two different pressure levels for the connected hydrogen storage vessel. Simulation results assess the EMS performance and robustness for the innovative integrated layout including the industrial symbiosis. Special attention is devoted to the performance improvement in terms of cost decrease, CO_2 emission decrease, and system efficiency increase.

Keywords: Renewable energy, intelligent control, plant integration, energy storage

NOMENCLATURE

AD	Anaerobic Digester
BES	BioElectrochemical System
CHP	Combined Heat and Power system
DMPC	Discrete Model Predictive Control
DLQR	Discrete Linear Quadratic Regulator
EL	Electrical
EMS	Energy Management System
ETN	European Turbine Network
EU	European Union
IES	Innovative Energy Systems
LNG	Liquefied Natural Gas
MPC	Model Predictive Control
NMSS	Non-Minimal State Space
O&M	Operation & Maintenance
PI	Proportional Integral controller
PV	PhotoVoltaic
RES	RenEwable Source
SME	Small Medium Enterprise
TH	Thermal
TRL	Technology Readiness Level

Variables

A, B, C	general matrixes for the MPC
c	cost [€]
E	Energy [J]
J	cost function [€]
J_{cost}	total operational cost [€]
k	generic variable for the MPC presentation
LHV	Low Heating Value [J/kg]
m	mass flow rate [kg/s]
M	mass [kg]
N	number [-]
Nc	control horizon [-]
Np	prediction horizon [-]
p	pressure [Pa]
P	Power [W]
Q, R	weight matrixes for the MPC
r	set-points by the Decision maker [W]
Sell	Selling-buying ratio [-]
Ts	sample time [s]

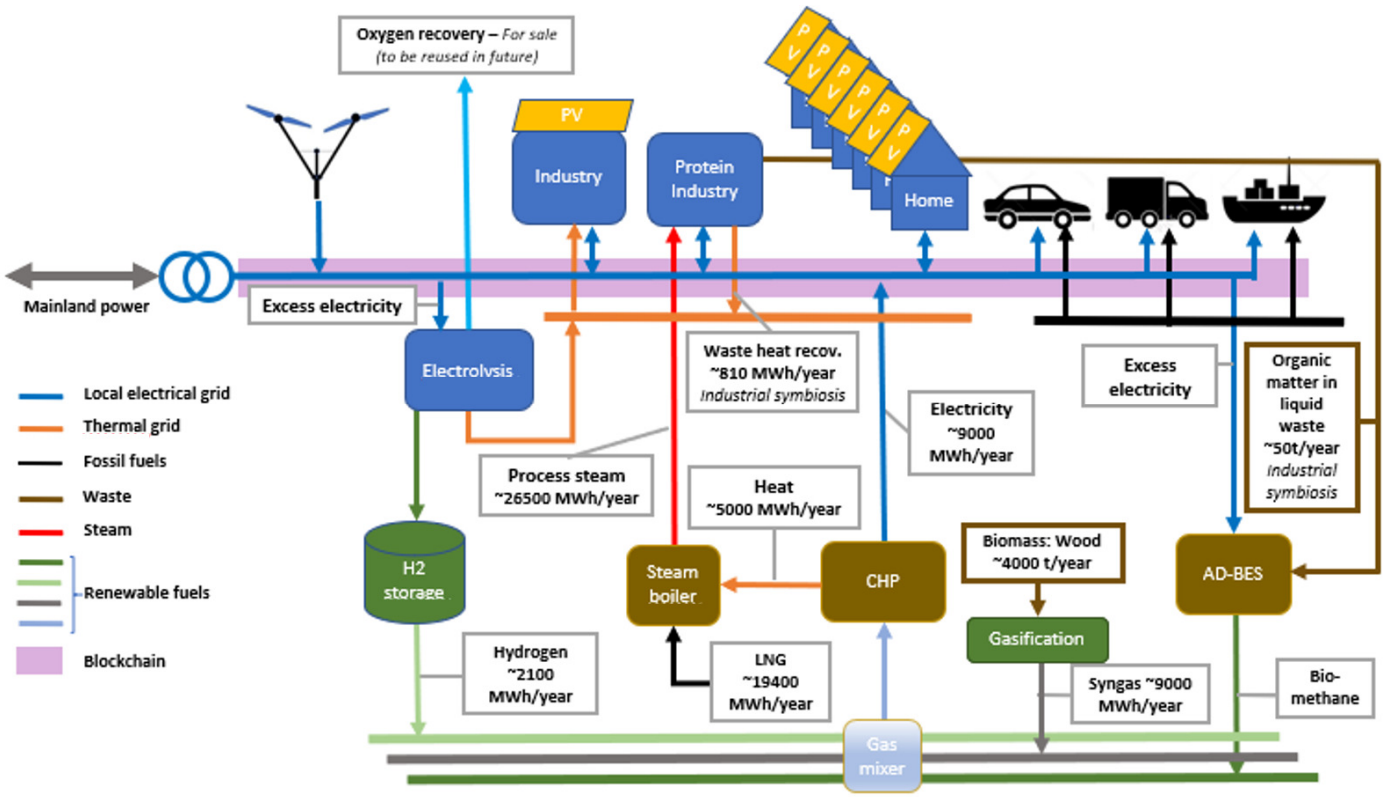

FIGURE 1: THE CONCEPT OF ROBINSON PROJECT FOR THE EIGERØY ISLAND

u	set-points or input variables for the system [W]
x	state variables [W]
y	output variables for the system [W]
η	efficiency [-]
Subscripts	
CHP	Combined Heat and Power
el	electrical
O&M	Operation and Maintenance
st	start-up
th	thermal

1. INTRODUCTION

In the recent years, the environmental issues [1] and the energy cost increase [2] forces both industrial and residential communities to consider innovative solutions for power generation. Starting from the benefits and the limitations of alternative (and not programmable) renewable sources [3], technology integration in smart grids [4] seems a solution with important potentialities to reduce CO_2 emissions, ensuring energy security conditions and acceptable costs [5]. Moreover, advanced grids with distributed generation technology based on different energy sources is an important option to have high flexibility level, avoiding large dependence on natural gas [6]. Moreover, to pursue the EU Green Deal objectives [7], as the international agreements on CO_2 emission decrease, the utilization of energy storage systems is essential [8]. In details, although different technologies could be considered (including batteries where effective), hydrogen generation and storage [9] seems a promising solution, also considering the related options (from high pressure vessels to metal hydrides or ammonia [10]). However, the choice of energy storage technology and the related overtime management remain critical issues due to the large amount of variables involved in the process [11]. First of all, it is important the system choice and dimension that is linked with costs, energy security, reliability, etc. [12]. Then, as the technology would be installed, it is important to define how to manage it during the time, avoiding energy missing conditions and minimizing the management costs [13].

Considering the scenario presented in the initial paragraph, it is clear that the development of a real-time software for the optimization of a polygeneration grid [14] is essential to include smart grids in the energy transition process. This tool needs to be simple for running in real-time mode, but with optimization capabilities. In this work, as in the ROBINSON project or in past activities, this tool is named Energy Management System (EMS) [15]. The EMS technology can range from very simple solutions (e.g. some if/else cases coupled with a prime mover ranking [5]) to very complex approaches using optimizers [16] or agent-based calculations [17]. In this work, considering the positive results obtained in previous activities including experimental

tests [17], the EMS is based on the coupling of a market function block (with a minimization algorithm and if/else cases) with a Model Predictive Control (MPC) tool that takes into account the dynamics of the generators avoiding a rigid connection between the optimizer and the physical systems [18]. Since this approach has been already testes at Technology Readiness Level (TRL) equal to 5 [17], in the ROBINSON project the demonstration in the Eigerøy island (Norway) is expected to reach TRL 7 [19].

Considering the needs of the ROBINSON project, the activity has been started with simulations in Matlab-Simulink including the models (software) of the necessary generators. Although the project activities will continue with experiments in the Innovative Energy Systems (IES) laboratory [20] at the University of Genoa, before switching to the demo site in Norway, this paper focuses attention on the modeling and simulation results obtained in Matlab-Simulink thanks to the development and the validation of almost black-box models for the generators. However, for the composition treatment (e.g. essential in the fuel mixer) and the hydrogen storage vessel, some approaches have been obtained from the TRANSEO tool of the University of Genoa [21].

Although several optimization tools have been developed with different approaches [22] (conventional analytical methods, evolutionary algorithms, hybrid intelligent, statistical models, etc.), in this work it is necessary to use a simple tool able to operate in a real-time mode with nonlinear problems. So, following preliminary calculations the "patternsearch" Matlab function was chosen to obtain a good compromise between reliability (to find global minimum, not local ones) and computational effort. Moreover, it is important to highlight that, in comparison with previous works (with traditional [23] and renewable sources [24], also including the climate condition effect [25]), the EMS of this work was developed with the real application objective. So, it needs to be operated in connection with the real system in real-time mode, with an important impact on the algorithm choice.

The main innovative aspects of this paper regards the management of different integrated generation technology (including the industrial symbiosis for waste resource recycle) with a robust EMS. It has (at the moment just with simulations) good perspectives to operate at high TRL level due to high robustness and important integrated performance in terms of cost decrease, efficiency increase and CO_2 emission saving. To the authors' knowledge, the robustness simulations presented in this paper are innovative because there are no similar analyses in the literature. However, they are essential results for such application at high TRL level.

2. THE ROBINSON PROJECT

The ROBINSON project, that has been started in October 2020 and will last to the end of September 2024 (except extensions), is part of the EU H2020 program [26]. It involves 18 partners, under the coordination of the European Turbine Network (ETN) including research centers, universities, companies (also SMEs) and local authorities. Although the project is quite complex with several objectives to be reached [19], in few words the main ROBINSON target is the demonstration in a real plant of a smart component integration for satisfy the local energy needs. Special attention is devoted to the integration of the renewable sources and to the industrial symbiosis (utilization of industrial waste for the local generation process). Although the demonstration is planned in the Norwegian island of Eigerøy involving the industrial symbiosis with the Prima Protein company, the project includes detailed analyses and experiments in the IES laboratory for the concept replication, starting from energy districts in Crete (Greece) and in the Western Islands (United Kingdom). However, the simulation tool and the related results included in this paper refer just to the Eigerøy island considering further publication opportunities for the other cases. Figure 1 shows the general layout of the ROBINSON concept applied to the Eigerøy island. The system includes different grids for electricity, heat, hydrogen, steam and other fuels (syngas and biogas). The demands regard electrical and thermal needs of houses, industries and vehicles. Moreover, the grid is mainly equipped with these technology: (i) 400 kW (electrical power) microturbine (CHP), (ii) 22 MW (steam) boiler, (iii) two 500 kW (consumed electrical power) electrolyzers, (iv) a very small anaerobic digester (<0.25 Nm^3/day of biogas) based on bioelectrochemical system (AD-BES) for using the industrial waste, and (v) a wood gasifier sized for about 70% of the fuel needed by the CHP, (vi) a 100 kW wind turbine, (vii) PV panels. Moreover, the grid includes a 40 m^3 pressure vessel for hydrogen storage, and a gas mixer for generating the proper fuel mixture for the microturbine. To complete the configuration, it is important to highlight that the thermal power produced by the microturbine (an A400 machine working in CHP mode [27]) is used to pre-heat the water for the steam generation. This layout solution was defined during the proposal submission to give the priority to the industrial symbiosis. So, no connection between the CHP thermal generation and the grid was included, to exploit all the CHP thermal energy for the boiler water pre-heating. However, since the ROBINSON project includes a workpackage on business cases and design improvement, it could be possible to have a different configuration on the thermal side for the demonstration (this is an ongoing activity). The component sizes were defined on the basis of these aspects: (i) the boiler was already present in the site (it was designed and installed in the past to satisfy the steam needs by Prima Protein), (ii) the CHP and the wind turbine sizes were chosen to cover an average electrical district demand (with several hours including an important grid charging), (iii) the electrolyzers were chosen considering the available sizes on the market and the hydrogen needs (as shown in these simulations the chosen size is able to generate the necessary EMS flexibility to maintain a minimum energy safety margin - 6 hours of autonomy with the CHP at maximum load plus a further margin from the empty condition), (iv) the hydrogen storage vessel size was chosen depending on the available space and the needs of guaranteeing at least 12 h of CHP autonomy at full charged condition).

This is the configuration that was considered in this work, as defined in the initial part of the project. So, although the

results shown here will be significant for the EMS development and testing, the further project development can produce significant changes in the layout (also considering other ongoing analyses in the project) moving the demonstration to a different configuration.

3. THE ENERGY MANAGEMENT SYSTEM

The Energy Management System (EMS) developed for the ROBINSON project needs to control the smart grid system in a robust way, integrating the inputs from other sources around it while aiming at the minimization of the costs, considering also the management of the hydrogen storage vessel. The EMS is basically constituted by a decision maker (the block called "Decision maker - Market function" in Fig.2) and an MPC. The necessary inputs are the power demands (also in real-time mode), the cost curves for the electricity market and the fuel costs. It is possible to consider also the hourly scheduling in case these data will be known.

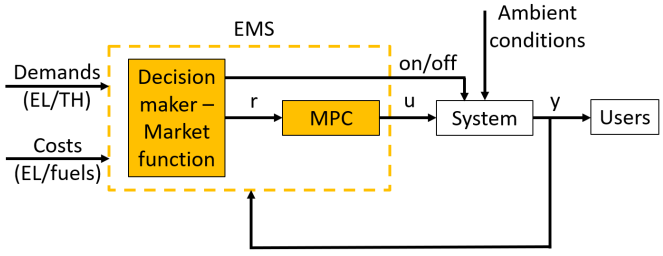

FIGURE 2: THE GLOBAL LAYOUT OF THE ENERGY MANAGEMENT SYSTEM

Basing on the demand curves, the Decision maker calculates the best strategy with a 15 minutes time step, defining the set points (r, in Fig.2) for the system in order to minimize the operational cost. This is done using an optimizer, described in section 3.1. Moreover, the Decision maker produces the Boolean on/off signals for the following system components: the CHP, the boiler and the electrloyzers. This is to perform component switch off in case this operation would be calculated as effective from cost minimization point of view. In case of "off" signals, the involved components are immediately switched off because the Fig.2 approach bypasses the MPC tool. The set point signals computed by the Decision maker then need to be used by a controller and passed to the system as actuators signals (u, in Fig.2). The system output (the generation for the users – y, in Fig.2) is the feedback for the EMS. These three vectors (r, u, and y) include in this work the following power set-points or measurements: the CHP electrical power, the boiler thermal power, and the electrical power of the electrolyzers.

In the final application, the controlled system (in Fig.2) will be the real energy generators of the ROBINSON demo. However, in order to set up the controller, it is fundamental to study it in a simulation environment, and this requires a model as accurate as possible. This is made through the development of data-driven models of each component of the system. These models are used to set up and test the EMS in the simulation environment, and then followed by an implementation in cyber-physical mode (future activity planned in the IES laboratory). More details on the component models are discussed in section 4 of this paper.

The controller is constituted by an MPC, which itself is split in the actual discrete-time MPC and an observer, that provides information on the system. A predictive control needs to have a model of the system itself in order to accurately predict the response of the real system and tune the best set point signals. So, it is necessary to know the actual state of the system. However, usually it is not possible to know every parameter of the system, thus an observer is used to estimate the state of the real system, using the measured outputs of it (y, in Fig.2). Thus, with information on the 15 min set points from the optimizer and the measured output of the system, the MPC is then able to communicate the actuator signals with a time step of 1 s (it is the global sample time of the simulation).

The interactions between the EMS and the simulated components are shown in Fig.3. As discussed in Section 4, the AD-BES and the gasifier are not directly interacting with the EMS because (due to their very slow response) they are supposed to be controlled to maintain constant the pressure in their gas outlet buffers.

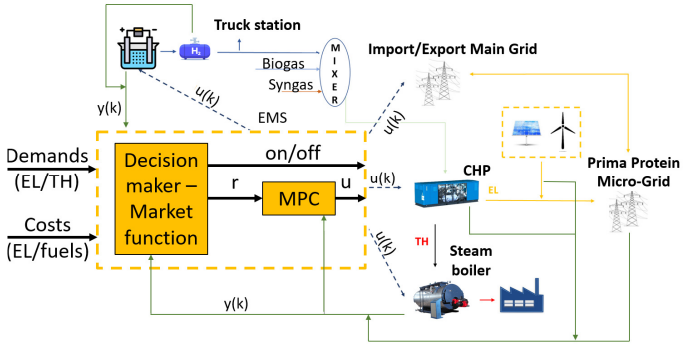

FIGURE 3: INTERACTION BETWEEN THE EMS AND THE SIMULATED COMPONENTS

3.1 Decision Maker - Optimizer

The decision maker is an on-line scheduler which implements an optimizer in order to find the best set point values given the state of the system and the demand and costs.

As previously introduced, the decision maker aims to minimize the total operational cost (J_{cost}) needed to satisfy the electrical and thermal demand, leading to an optimized curve of the set points every 15 minutes. To do that, the optimizer receives the electrical and thermal demands, the renewable energy production, the electricity and fuel costs, together with the characteristics of the boiler and the CHP. The optimization variables (the decision variables) are the electrical power exchanged with the grid ($P_{el_{grid}}$) and the electrical power produced by the CHP ($P_{el_{CHP}}$). The objective function is fully presented by Eqs.1, 2 and 3 that are necessary to show how the different parts are calculated. The Operation & Maintenance costs and the start-up operation impact are included in Eq.1, as

previously presented in [28]. Finally, no thermal energy cost is included in Eq.1 because it is considered as an internal production and consumption, not generating any cost.

The fuel mass flow needed to achieve a certain CHP electrical power is computed, starting from the rated values, using the consumption curves of the specific device. If power is purchased from the grid, the cost is based on the purchasing price, otherwise if the power is sold to the grid, the electrical power is multiplied by the selling price value (purchasing price per the selling-buying ratio). So, with this approach it is possible to use a selling price lower than the buying one (as it happens in some electricity contracts). The optimization is based on the constrains of Tab.1. Moreover, the tool receives also the constraint related to the electrical power balance: the electrical power bought (or sold) from the grid is the difference between the electrical demand and the electrical production by the CHP (all values as power). If the sign is positive the system is buying electrical energy from the grid, while in case of negative values, the system is selling electrical energy to the grid (obtaining an economic income that is taken into account).

$$J_{cost} = (c_{el} + c_{O\&M}) \cdot P_{el_{grid}} + c_{fuel_{CHP}} \cdot m_{fuel_{CHP}} + c_{st} \cdot N_{st} \quad (1)$$

$$m_{fuel_{CHP}} = f\left(P_{el_{CHP}}, LHV_{CHP}, \eta_{CHP}, T_{amb}\right) \quad (2)$$

$$c_{el} = \begin{cases} c_{el} & if\ P_{el_{grid}} > 0 \\ c_{el} * Sell & if\ P_{el_{grid}} < 0 \end{cases} \quad (3)$$

Since the problem is nonlinear (due to the CHP efficiency curve shape), the optimization algorithm is nonlinear. In details, it is the "patternsearch" Matlab function [29,30] operated with the following parameters: initial state vector array, linear equalities, linear inequalities and lower/upper bounds of the two decision variables. The initial state is zero for both variables, the linear equalities regard the link between the electrical power values (CHP generation, grid and CHP maximum), the inequalities express that the sum of these variables must be lower than the maximum (CHP+grid) and the lower/upper bounds are reported in Table 1. This optimization function was chosen because it was the best one to calculate the global minimum avoiding risks of obtaining local solutions. This decision comes from result comparison with other algorithms based on the gradient method.

The result of the optimization is thus the 15-minutes interval scheduling, resulting in a Boolean indication whether it is convenient to produce electricity with the CHP and sell it to the grid, if the optimal power of the CHP is higher than its minimum value, or if it is convenient to buy the electricity from the grid, in case the optimal power of the CHP is lower than its minimum value.

This is then applied in a logic which objective is to follow the thermal demand of the system, as shown in Fig.4. There are three possible behaviors for the CHP: if the thermal power demand is lower than the minimum provided by the CHP, if the thermal power demand is between the minimum and maximum that can be provided by CHP, and the case in which an integration with a boiler is necessary to satisfy the thermal load.

TABLE 1: CONSTRAINTS OF THE SYSTEM, USED BY THE DECISION MAKER

Parameter	Min value	Max Value	Unit
CHP EL Power	70	400	kW
Grid EL Power	-2000	2000	kW
Boiler TH Power	2200	22000	kW

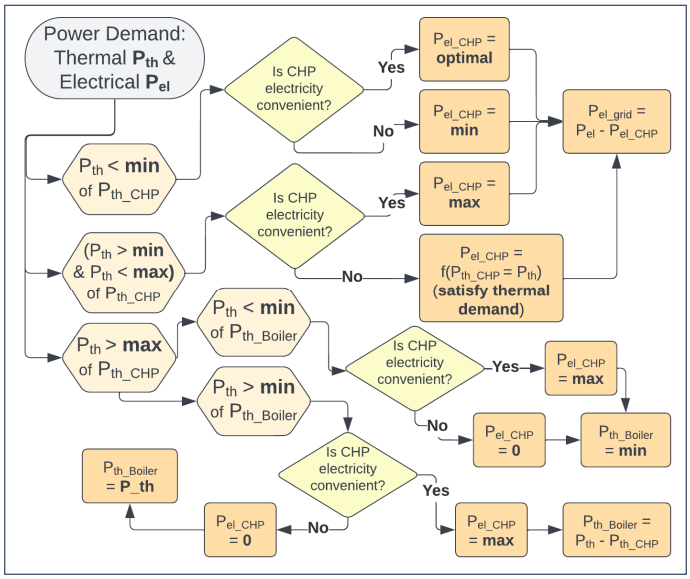

FIGURE 4: FLOWCHART LOGIC OF THE DECISION MAKER

3.2 Model Predictive Control

The model predictive control (MPC) system was developed following the procedure suggested in the book by Wang [31]. This controller is a constrained multi-input multi-output MPC, constituted by the actual discrete-time MPC and the integrated observer, used to estimate the state of the system. Its role is to control the system, by computing the values of the actuator variables, given the information on the setpoints from the decision maker, and the state of the system from feedback of measured values of the system.

The initialization consists in the definition of the time windows for the prediction horizon (N_P = 40 steps) and for the receding control horizon (N_C = 1 step), together with the definition of the sample time of the discrete system (Ts = 1 s). The prediction horizon was set equal to the number of steps (1 step = 1 second in this case). It was set equal to 150% of the bigger characterization time constant; then the controller could predict the operations of all prime movers considering their transients. The receding horizon was set equal to 1 step. Then, the information on the controlled plant, constituted by the CHP turbine and the steam boiler, is needed. A linearized state-space representation of the plant is then used, and passed to the observer; then, it is transformed into an augmented state-space model (matrices A,B,C): it can be based on the differences of the

state variables (Δx) and of the input variables (Δu), as shown in the Eq.4. After that, the knowledge of the augmented state-space system, as described, is reordered to be parametrically passed to the actual MPC, together with the constraints on the variables.

$$\begin{cases} \begin{bmatrix} \Delta x(k+1) \\ y(k+1) \end{bmatrix} = A \begin{bmatrix} \Delta x(k) \\ y(k) \end{bmatrix} + B\Delta u(k) \\ y(k) = C \begin{bmatrix} \Delta x(k) \\ y(k) \end{bmatrix} \end{cases} \quad (4)$$

When running the code, the controller receives the set points from the decision maker, and the measured values ($y(k)$) from the plant, giving the control signal as an output. Inside the controller, the observer receives the control output from the actual MPC, the estimated state of the system, and the measured values from the plant, to which it applies a Kalman filter. From this information, together with the knowledge of the state-space representation of the system, the observer computes a new estimate of the state of the system. This is received by the actual MPC, which computes a new value for the control variables, which are then passed to the plant and sent in feedback to the MPC and the observer too, to be used in the next step.

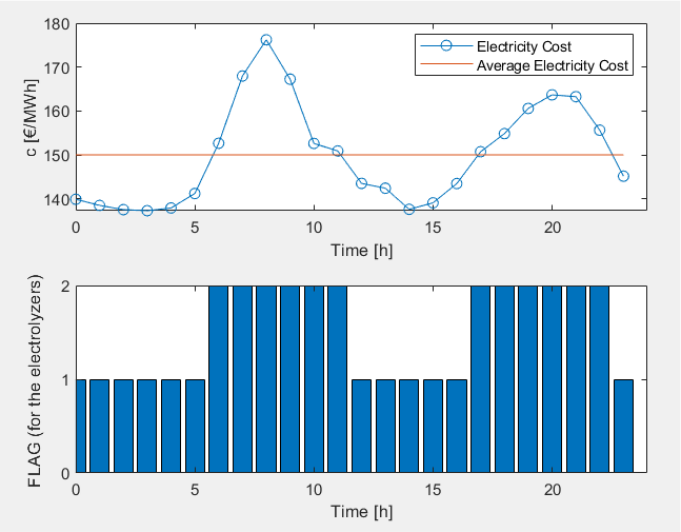

FIGURE 5: ELECTRICITY COST AND HYDROGEN PRODUCTION (DAILY SCHEDULING)

In this work, the MPC architecture is based on two functions: one for the discrete model predictive control (DMPC) and one for the observer, according to the velocity form presented here [32]. The model developed for the control is based on augmented state-space representation, i.e. Non-Minimal State Space (NMSS) (Eq.4) [31]. The observer is used to estimate the state of the system at each time step, to be fed back to the DMPC dynamic model for the following iteration. This non-minimal representation is detectable and stabilizable if the original model is detectable and stabilizable and has no transmission zeros on the unit circle. The integration within the MPC is performed through the application of the Laguerre network. It is used to simplify MPC computation by adding tuneable parameters. In literature, Laguerre functions were used to describe the pulse response of dynamic systems – it is possible to describe dynamic behaviour of target system through this method. One of the advantages of MPC is linked to the possibility to tune controller response based on weights associated to control variables. Here, cost function is based on Discrete Linear Quadratic Regulator (DLQR) architectures, which are used to be as Eq.5, with Q and R weight matrices, x is the state of the system, and u is the control signal. DMPC algorithm includes constraints on absolute value of plant inputs u and their rate of change Δu.

$$J = \frac{1}{2} x^T Q x + u^T R u \quad (5)$$

3.3 Hydrogen management

The hydrogen production depends mainly on the electricity price, thus the main schedule of the production is made off-line, and it results in a daily scheduling with an 1 hour time span, with two possible behaviors, as it can be seen in Fig.5. If the electricity price is lower than the average one, the electrolyzers will run at design point (flag 1), otherwise the electrolyzers will run at part-load (flag 2). In details, Fig.5 reports the electricity cost variation for a day in the month of November 2021 for the Eigerøy island. This approach was chosen for the management of the electrolyzers due to the necessity to have a scheduling based on the electricity cost values of the entire day (these can be forecasted on the basis of the previous day data and on other information, such as the day type) [33]. So, when the electricity cost is low, the electrolyzers at maximum load exploit the price situation trying to recharge the storage vessel. On the other hand, when the electricity cost is high the electrolyzers are managed by a devoted controller to reach the minimum pressure set-point, because it is not convenient to do the vessel full re-charging.

Given the scheduling based on price, the actual hydrogen management will follow the pressures of the storage, using an on-line scheduler and a dedicated MPC. In particular, the target pressures for the hydrogen storage can be 40 bar (in case of low electricity price) or 22 bar (in case of high electricity price), while the maximum and minimum values are 42 bar and 10 bar. These numbers were chosen on the basis of the data provided by the proposed manufacturer (design and maximum pressure values) and to ensure a good energy safety margin (22 bar set-point guarantees 6 hours of autonomy with the CHP at maximum load plus a further minimum margin for a further safety from the empty condition). For sure different values could be used depending on the energy safety level that is necessary to guarantee on the hydrogen storage side.

The control of the electrolyzers is structured with this approach: an on-line scheduler receives the off-line daily scheduling and the target pressure of the H_2 storage, and computes the set points of the absorbed electrical power. In case of flag 1 (low electricity price), if the pressure of the storage is lower than 90% of the maximum value, the electrolyzers work at design point; instead, if the pressure is between 90% and 96% of

the maximum value, the power of the electrolyzers is controlled by the dedicated MPC; finally, if the pressure is higher than 96%, the electrolyzers are switched off (the 90%, 96% values were proposed after trials with the objective to avoid risks of pressure values higher than the maximum constraints). Instead, in case of flag 2 (high electricity price), the target pressure will be equal to 22 bar, and if the pressure of the storage is higher than this value, the electrolyzers are switched off; otherwise, the power of the electrolyzers is controlled by a dedicated MPC.

The models of the electrolyzers, two identical working in parallel, receive an electrical power set point and compute the efficiency, and the production in terms of H_2 and O_2 mass flow rates, with a dynamic first-order delay. The mass flow rates are then used by the hydrogen storage model, to compute the pressure of the storage itself, having assigned a certain volume (40 m^3). The outlet mass flow rates from the storage are determined by the utilization for transportation and by the need of the gas mixer to satisfy the desired percentage of hydrogen in the CHP fuel composition. On the transportation side, trucks using H_2 as fuel are charged, and the tank of the trucks can hold up to 32 kg of H_2; a further constraint is that the charging process must not lead to a pressure in the storage lower than the minimum allowable. Thus, the outlet mass flow rates of hydrogen are computed and the MPC takes them into account to regulate the absorbed powers of the electrolyzers to achieve the target pressures of the storage vessel.

4. COMPONENT MODELS

Although in the real demo (on the Eigerøy island) the necessary software will be just the EMS (the content in the dotted line in Fig.2), at simulation level it is necessary to have component models for all the prime movers. These are: the CHP, the boiler, the renewable-source generators (solar photovoltaic panels and a 100 kW wind turbine), and the electrolyzers (N.2 500 kW units in this analysis). Moreover, the modelling activity included also the hydrogen storage (a pressure vessel) and the fuel mixer. For the electrical side, the grid power is constrained to balance the system for every sample time of the calculation (it provides the missing demand or receives the excess of power generated by the CHP). Moreover, it provides also the electrical power for the electrolyzers. No models have been used for the AD-BES and the gasifier because they are very slow response devices. So, they are supposed to be controlled to maintain constant the pressure in their gas outlet buffers (devices installed to compensate the system slow dynamic response and to be able to deliver to the mixer all the gas needed for the CHP).

For the models implemented in this analyses, detailed tools are not necessary because they have to calculate just the global performance values (such as electrical and thermal power and fuel mass flow rate for the CHP) in design and off-design and dynamic modes. So, the CHP, the boiler, the renewable-source generators, and the electrolyzers have been modeled with black-box approaches. When the link between set-point and performance is the result of complex processes (e.g. for the CHP) data-driven approach (black box) was considered, performing the linear interpolation between experimental performance data provided by the manufacturers. The time-dependent behavior is obtained with dead-time and a first-order delays. These time-constants were set on the basis of data provided by the manufacturers or obtained from literature. This approach, although affected by errors, is a good compromise between the needs of fast calculations and a reasonable accuracy. Moreover, it is important to highlight that the results presented here are essential to evaluate the general EMS performance and robustness, while minor adjustments will be possible during the demonstration.

In details, the model of the A400 turbine includes part-load curves, correlations and dynamic manufacturer characterization (deadtime and first order delay constant) to calculate off-design and transient behavior. The steam boiler model computes both transient and part-load operations using manufacturer's data and literature off-design characteristic curves. The equation below defines the efficiency at part-load operations in agreement with an existing device [34] (Eq.6).

$$\eta = \eta_{nom} * \sqrt{(1 + load\%)/2} \quad (6)$$

The wind turbine model calculates the power generation with the performance curve by the manufacturer. The model input is the wind speed, while the output is the generated electrical power. Also the PV panels are modelled with a simple approach: irradiation per active area per panel efficiency.

The model of the electrolyzers includes part-load performance curves and dynamic behaviour literature data [35], to calculate the transients and the steady-state operations. The electrolyzer dynamic response is based on a first order delay, as presented in [36] and confirmed by the manufacturer.

Although the specific data for the performance curves used in this work are not always available due to confidentiality reasons, the EMS simulations could be replicated with literature data of similar machines. While differences would be present, the general management approach and the optimization effectiveness would be easily replicated.

A specific attention was considered for the hydrogen storage vessel and the fuel mixer. Due to the necessity to implement some physical-based dynamic equations (especially the continuity and the energy equations in dynamic conditions for multi-input and multi-output vessels), they have been developed starting from the TRANSEO tool [21]. Moreover, due to the heat exchange necessity, the adiabatic plenum concept has been integrated with the 0-D heat exchange, as previously developed in the TRANSEO component named "pipe" [36]. For the flow composition (and the calculation of the related properties), a simplified approach has been used on the basis of the real-time version of the TRANSEO tool (as presented in [37]). So, it was possible to start from a well validated approach that was used for dynamic simulations in several cases. For instance, in [38] the pressurization time was calculated thanks to the TRANSEO pressure vessel in good agreement with the experimental data. Moreover, in [37] the composition management has shown results well matching the experiments, with the accuracy order

of magnitude expected in these real-time models including several components.

4.1 Component model validation

The models of components were validated considering both data provided by the manufacturers or available from previous tests. Moreover, some components were validated in previous works, as discussed before.

As an example of different cases, this section reports the validation in dynamic conditions for the 22 MW boiler and for the CHP. Fig.6 shows the boiler dynamic response (in terms of thermal power) related to a set-point step. Although the experimental data (±3% accuracy) provided by Prima Protein show several oscillations, the model is able to calculate the general trend with a good agreement.

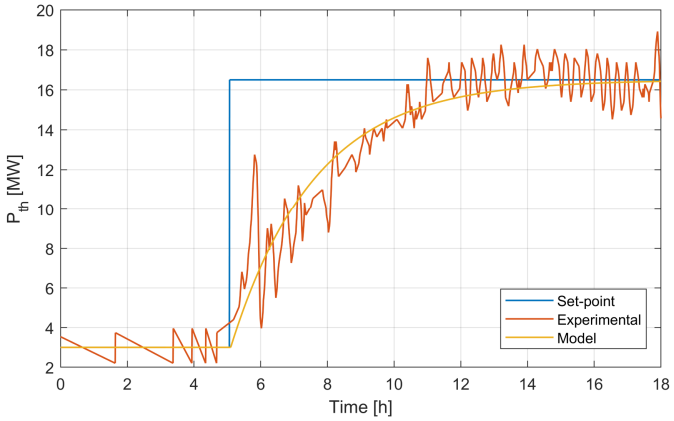

FIGURE 6: VALIDATION OF THE BOILER MODEL

Since for the A400 machine no data are available in dynamic mode, the model validation was performed considering experimental results of the T100 machine that is available in the IES laboratory by the University of Genoa. This is useful because the CHP model implemented here is a black box tool: interpolation of performance maps, dead time and first order delay. So, although the T100 turbine is quite different from the A400 machine, with this simulation approach the CHP change is performed with different implemented maps and time constants.

Considering this tool validation, Fig.7 shows a good agreement between the calculated results and the experimental data for the electrical power produced by the T100 microturbine (±1% accuracy) following a large set-point step (from 20 kW to 60 kW). Although the model is not able to calculate the oscillations, it matches correctly the general time-dependent behavior, as requested for the calculations with the EMS. In details, although the power overshoot cannot be obtained with this simplified modelling approach, this is negligible considering the hour time scale of the planned simulations. Moreover, thanks to the connection to the electrical grid, such additional generated power can be provided to the grid in case higher than the demand. Errors related to the missing overshoot simulation are negligible in the global performance calculations. In this case, Fig.7 presents a time constant equal to 23 s for a maximum power rate of 2 kW/s. Although this time-constant was updated for the A400 turbine, for confidentiality reasons, the details cannot be provided here.

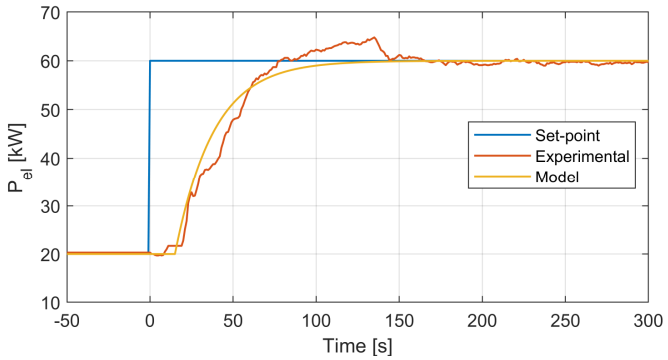

FIGURE 7: VALIDATION OF THE CHP MODEL

5. RESULTS AND DISCUSSION

The simulation results presented here were obtained with these mentioned validated component models interacting, as in Fig.2 with the presented EMS. As presented before, the analysis was performed for the data related to a day of November 2021. The electricity cost trend was already presented in Fig.5, while for the syngas a cost of 5 €/MWh has been considered (it is mainly related to the wood cost). For the LNG (the fuel for the boiler) a cost of 150 €/MWh was considered. For the hydrogen flow used for vehicle charging, N.2 13.3 g/s demand periods were included for a duration of 2400 s each. The first charging event is at 5 a.m. while the second one at 11:15 a.m. to simulate a possible future real situation. Although no data are available on this side because related to future operations, this could represent a typical truck re-charging. Different re-charging operations can be considered in future works on the basis of statistic data. Another assumption regards the hydrogen percentage in the CHP fuel. At the moment, this was fixed to 30% in volume for all the simulations. So, depending on the CHP load (and its fuel consumption calculated by the model) this fixed percentage allows to calculate the amount of hydrogen for the CHP to be taken from the storage vessel. Finally, the electricity selling-buying ratio was 1 for the simulations discussed in this section.

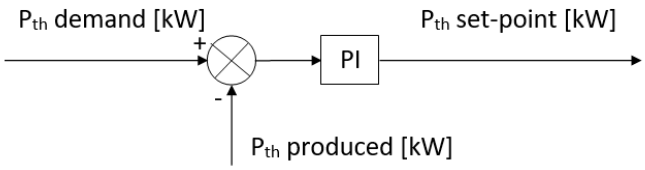

FIGURE 8: PI CONTROLLER FOR THE BOILER IN THE NO EMS CASE

5.1 EMS comparison with a system standard management

An initial result that is reported here regards the comparison of the system management if operated with the EMS against a

standard management approach. Since the plant is not available/installed yet, it is not possible to compare the EMS results against an existing standard procedure. So, for the "No EMS" management a simple approach is implemented in the software to consider operations on the systems that could be performed without any smart tool. This reference approach (named "No EMS" in the figures) means that the system is managed in this way: (i) the CHP is simply operated to satisfy the electrical demand, (ii) the boiler is switched on when the thermal demand is higher than what can be satisfied with the CHP (since the boiler has a low response performance and 2.2 MW of minimum load, the set-point signal is provided to the device through a PI controller – see Fig.8 for details), (iii) the two electrolyzers are maintained at minimum load for the entire simulation (considering that with the EMS they are managed at higher load for some part of the simulation or switched off for another part). The management at minimum load for the electrolyzers in the "No EMS" case was chosen to have a reference operation that does not require any control or smart operation. Moreover, this is a hydrogen generation able to maintain the vessel in the 22-40 bar range (large discharged condition would generate comparison difficulties with the EMS case).

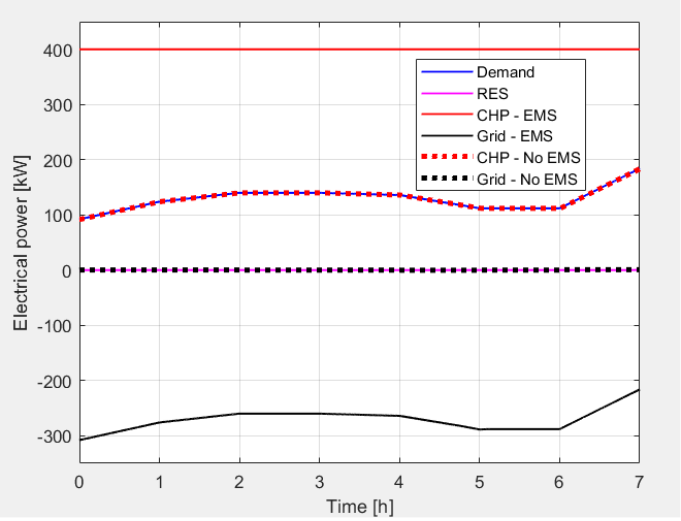

FIGURE 9: EMS VS NO EMS (ELECTRICAL POWER)

Due to the system characteristics (a 400 kW CHP with a 22 MW boiler), instead of simulating the entire day (where in a large part of the analysis the performance is driven by the boiler) attention was focused on the initial 7 hours (from midnight to 7:00 a.m.). This is a period with the factory start-up, so with an important part of the electrical demand lower than the CHP maximum and the boiler ignition. Moreover, the simulation of the entire 24 hours is presented in the next sub-section. Due to the hours that were chosen, no generation by PV panels is present. Moreover, due to low wind conditions in this period, also the contribution by the wind turbine is null (as shown in Fig.9). Since the syngas cost is very low in comparison with the electricity one, the EMS maintains the CHP at its maximum for all the 7-hour test. This is a good approach because the electrical energy not consumed to satisfy the district demand is sold to the grid obtaining a significant profit. Moreover, Fig.9 shows that in the no EMS case, the CHP simply matches the electrical demand.

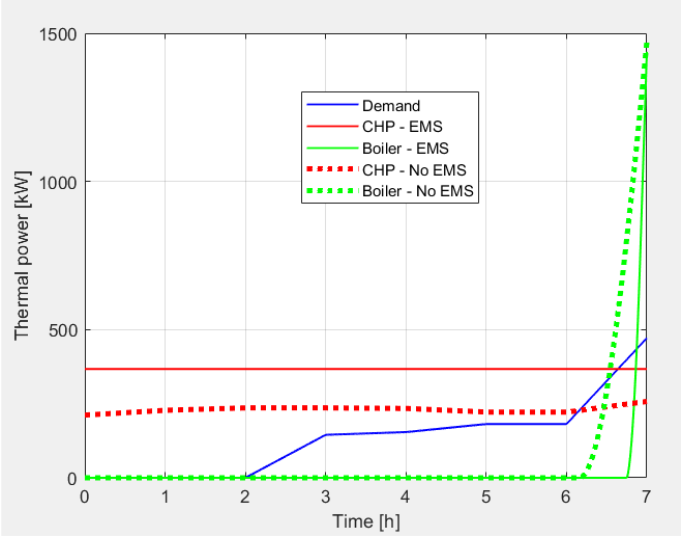

FIGURE 10: EMS VS NO EMS (THERMAL POWER)

On the thermal side (Fig.10), the CHP produces the necessary thermal power for more than 6 hours (since at the moment the system does not include a thermal storage, the generation excess is dissipated). The excess of thermal power is more significant in the EMS case because the CHP is at its maximum. Finally, when the CHP is not able to satisfy the thermal demand, the boiler is switched on: due to the EMS coupled to the MPC tool the optimized case is more effective because the boiler switch on is delayed of about 30 minutes (with significant fuel saving) and has a faster increase trend in comparison with the no EMS case.

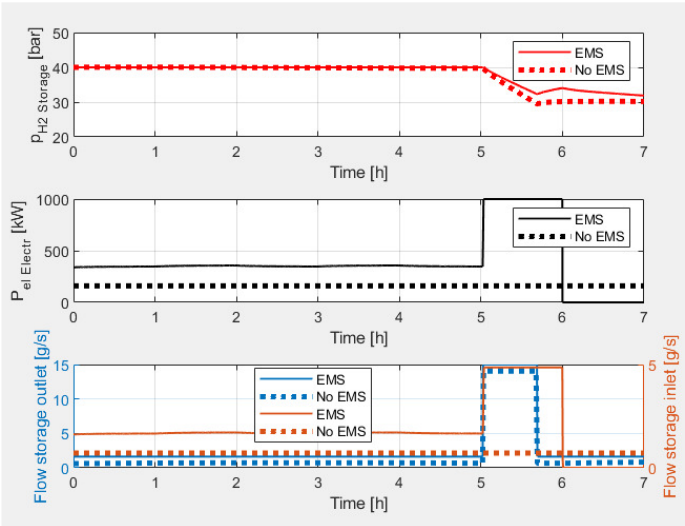

FIGURE 11: EMS VS NO EMS (HYDROGEN GENERATION, STORAGE AND UTILIZATION)

For the hydrogen storage point of view (Fig.11), in both cases the pressure decreases during these 7 hours due to the consumption for truck charging. However, while the EMS increases the set-point of the electrolyzers when the electricity cost is lower than the average, the no EMS case does not exploit this economic benefit. On the other hand, since the no EMS case is not able to switch off the electrolyzers, the pressure vessel show a slow recharging phase that starts at the end of the truck charging. In both cases the hydrogen pressure vessel remains in the 22-40 bar range without any risk of empty conditions.

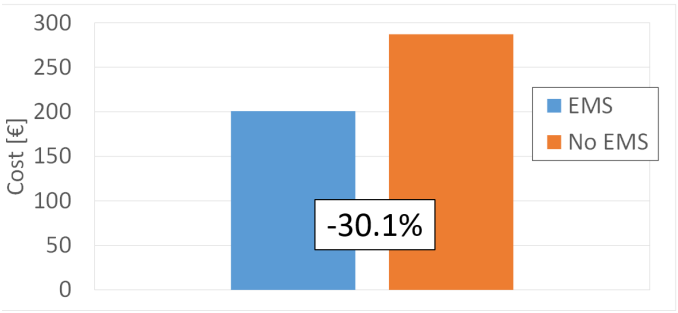

FIGURE 12: EMS VS NO EMS (VARIABLE COST COMPARISON)

Following the detailed analysis, a comparison of some global parameters is reported here. Since the optimization objective is the cost minimization, Fig.12 starts to show the comparison of the variable costs related to this 7-hour simulation. Since no specific data are available from the manufacturers for the component O&M costs, literature values were considered: 0.015 €/kWh for the CHP [39], 1.5% of the capital costs for the electrolyzers [40]. Due to the simulation aspects (no CHP on/off operations and boiler operations shorter than 1 hour) negligible O&M costs were considered for these aspects. Fig.12 shows a significant cost decrease (-30.1%) obtained with the EMS application. This is mainly due to the choice to operate the CHP at its maximum to obtain cost saving from the electrical energy selling. Moreover, the delayed switch on of the boiler produces a fuel saving on the thermal side.

Although the objective is the cost minimization, the global performance analysis shows positive effects also on other parameters, such as the efficiency values (Fig.13). For the efficiency point of view, attention is focused on the electrical side because on the thermal side the efficiency is driven by the boiler who is 1-2 orders of magnitude size larger than the other devices. So, the first-principle total efficiency remains very close to the boiler thermal one when this device is used (in this simulation it has a variation lower than 1.5%). So, Eqs.7 and 8 show the two types of electrical efficiencies that are compared here, expressed in terms of the energy values (produced, consumed or stored) in these 7-hour simulation. The fuel energy that is at the denominator (or a denominator addendum) in both equations is calculated doing the sum for every simulation second of the products of the fuel mass flow rate per the mixture lower heating value (calculated in the mixer). Moreover, Eq.8 shows that the system electrical efficiency includes also the hydrogen consumed for the truck charging ("users" subscript) and the hydrogen storage balance (in case of pressure decrease in the hydrogen vessel this term would be negative to take into account that the consumed hydrogen would be produced again in the following hours or days).

$$\eta_{el_{CHP}} = \frac{E_{el_{CHP}}}{E_{fuel_{CHP}}} \tag{7}$$

$$\eta_{el_{system}} = \frac{E_{el_{CHP}} + E_{H2_{users}} + \Delta E_{H2_{storage}}}{E_{fuel_{CHP}} + E_{el_{grid}}} \tag{8}$$

The performance comparison in terms of electrical efficiency is shown in Fig.13. Due to the utilization of the EMS that operates the CHP at the nominal condition, this microturbine has a significant electrical efficiency increase (35.3%). Moreover, also from the system point of view, including the EMS operations on the hydrogen system side, Fig.13 shows an efficiency increase of 41.6%.

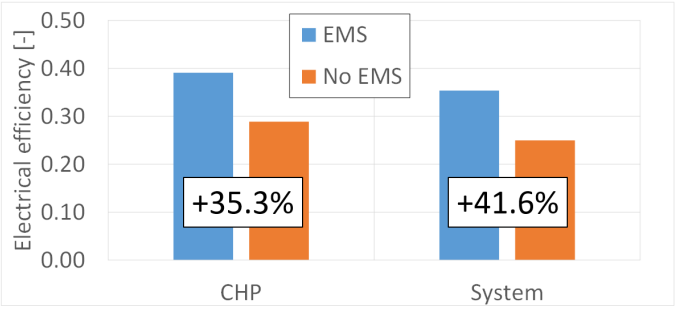

FIGURE 13: EMS VS NO EMS (ELECTRICAL EFFICIENCY COMPARISON)

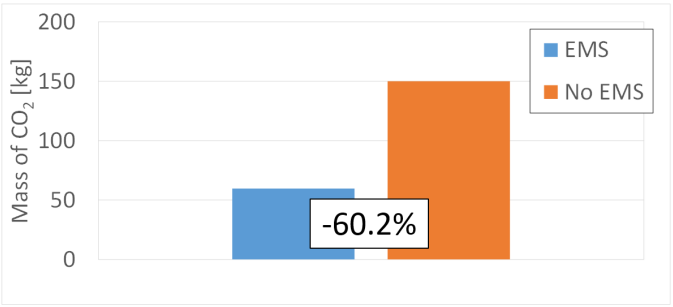

FIGURE 14: EMS VS NO EMS (CO_2 EMISSION COMPARISON)

The EMS has a significant impact on the CO_2 emissions related to this 7-hour simulation. These emissions are calculated as in Eq.9 with the sum of the mass of CO_2 produced by: the boiler combustion, electrolyzer operations (considering the electrical energy consumed from the grid), the energy generation bought from the grid (if this happens), the hydrogen storage change. It is important to highlight that the CO_2 emitted from the syngas/biogas combustion is considered null, because it comes from a renewable source that in case of not utilization would

produce the same amount of CO_2 in a rubbish dump. Moreover, since the grid electricity from fossil fuel is just the 2% of the entire amount, the CO_2 generation is mainly driven by the boiler that is fuelled by LNG.

$$M_{CO2_{system}} = M_{CO2_{boiler}} + M_{CO2_{electrolyzers}} + M_{CO2_{grid}} + \Delta M_{CO2_{H2\ storage}} \quad (9)$$

The performance comparison in terms of emitted CO_2 is reported in Fig.14. Also in this case, the EMS produces a positive effect (with an important environmental impact) obtaining a CO_2 emission decrease of 60.2% for this 7-hour simulation.

5.2 Simulation to assess EMS robustness

To assess the EMS robustness, a 24 h simulation was performed considering the entire data of Fig.5. As example of wrong measurements (due to probe errors or cyberattacks) the following events were included: (i) the measured CHP thermal power was equal to -50 kW for 1 h started at 4:00, (ii) the measured boiler thermal power was equal to -1.0 MW for 1 h started at 9:00, and (iii) the measured pressure in the hydrogen storage vessel was equal to -1 bar for 1 h started at 16:00. An initial check to prevent instability is related to saturation blocks. So, both CHP and boiler thermal power values were limited to 0 kW and the hydrogen vessel pressure to 1 bar (absolute pressure) because lower values are not acceptable from physical point of view.

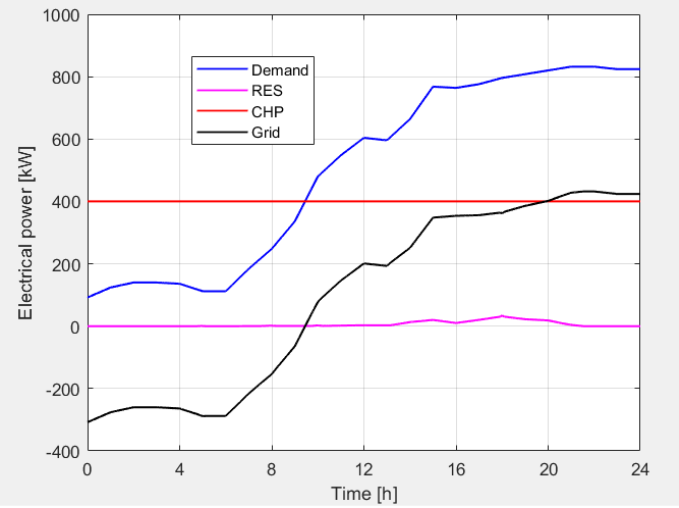

FIGURE 15: EMS ROBUSTNESS ASSESSMENT (ELECTRICAL POWER)

From the electrical side, the EMS operates the CHP at the maximum power (400 kW) for the entire simulation (Fig.15). So, the EMS continues considering the solution (already described for the initial 7 hours) for all the 24 h (also when the electrical demand reaches values higher than the CHP maximum). In this case the demand is significantly covered by the grid. It is important to highlight that during the afternoon the system has some electrical power from the renewable sources (specifically the wind turbine), up to 33.6 kW. This reduces a bit the energy that needs to be bought from the electrical grid. From the EMS robustness point of view, Fig.15 shows that the mentioned measurement errors have not any influence for the CHP management and this is well visible on the electrical side.

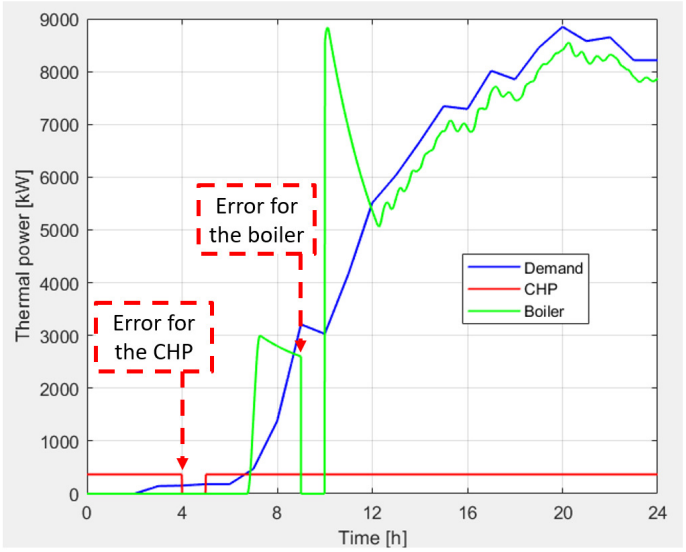

FIGURE 16: EMS ROBUSTNESS ASSESSMENT (THERMAL POWER)

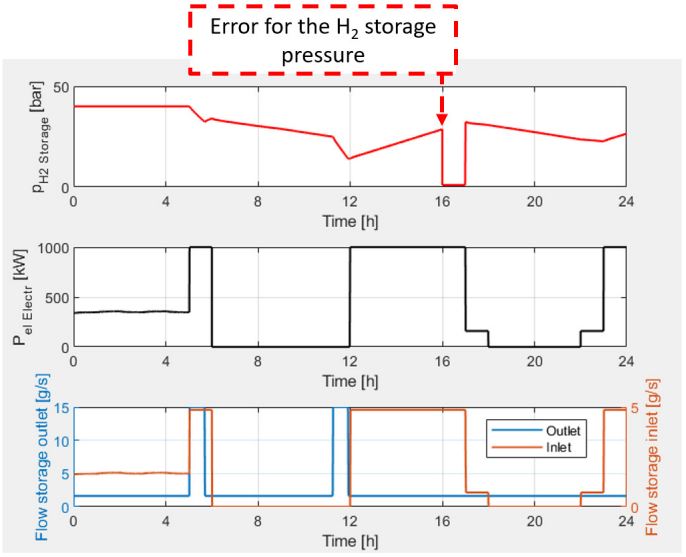

FIGURE 17: EMS ROBUSTNESS ASSESSMENT (HYDROGEN GENERATION, STORAGE AND UTILIZATION)

The measurement errors are visible on the thermal side (Fig.16). Although these introduce important errors in global parameter calculations (that in this case are not evaluated), no significant problems are reported in the component management. The only strange behaviour regards the boiler that is moved to a very high power generation after the measurement error because the set-point is increased too much to try to compensate the missing thermal power (from the measurement). However, in

about 1 hour the EMS is able to reduce the produced power to values in agreement with the demand (Fig.16 after 12:00 time).

Finally, Fig.17 shows the EMS robustness aspects on the hydrogen system side. While the errors on the thermal measurements have no effects here, also the large error in pressure vessel measurement is not producing critical problems. Since immediately before the error the vessel pressure is low (about 23.4 bar), the electorlyzers continue to be operated at the maximum (2 X 500 kW) without any discontinuity. For sure in case of a pressure value close to the maximum, the EMS would be not able to prevent damages from overpressure. So, in this case probe redundancy (and a safety system not accessible in online mode – to avoid risks in case of cyberattacks) would be important.

6. CONCLUSION

The core of this work regards the EMS development and the related simulations with models (software) for the system components. In details, the software (in Matlab-Simulink) includes the models for: a 400 kW CHP (the A400 microturbine), a 22 MW boiler for steam generation, N.2 500 kW electrolyzers, a connection with the electrical grid, some renewable sources (PV panels and wind turbine), a pressure vessel for hydrogen storage and a fuel mixer. The gasifier and the AD-BES for the industrial symbiosis are supposed to be controlled to maintain constant the pressure in their gas outlet buffers. The main results obtained in this work are presented in the following points.

- The EMS technology, already proposed in [17], was converted considering the final demonstration target. It was implemented on the basis of the integration of a constrained cost minimization problem with the hydrogen storage scheduling.
- Since the component models are simplified tools based on interpolation of data, deadtime and first-order time constant, the validation activity was an important step for obtaining reliable results. For the validation results reported here, the CHP and boiler models were able to calculate the general time-dependent trend in good agreement with the experimental data.
- The EMS/No EMS comparison simulations showed (for the 7-hour analysis) interesting performance increase when the system was managed by the EMS: -30.1% variable costs, +41.6% electrical efficiency, and -60.2% for the CO_2 emissions.
- The robustness simulations (considering measurement errors in the CHP thermal power, the boiler thermal power, and the hydrogen vessel pressure) sowed good EMS behavior: no instabilities due to these errors and optimal recalibration performance after the measurement error removal. These are essential aspects for the planned demonstration at TRL equal to 7.

Considering the positive results presented here, the EMS is ready for the next steps planned in the project: the laboratory tests in cyber-physical mode (a sort of intermediate test between simulations and real operations, using physical systems and simulation models in the same test [18]) and the demonstration in the Eigerøy island [19].

ACKNOWLEDGEMENTS

This project has received funding from the European Union's Horizon 2020 research and innovation programme under grant agreement No 957752. This paper reflects only the authors' view and the Research Executive Agency and the European Commission are not responsible for any use that may be made of the information it contains.

REFERENCES

[1] Green, R., Gill, E., Hein, C., Couturier, L., Mascarenhas, M., May, R., Newell, D., Rumes, B., International assessment of priority environmental issues for land-based and offshore wind energy development. Global sustainability, 5 (2022) article n. 14.

[2] Muñoz, P., Franceschini, E.A., Levitan, D., Rodriguez, C.R., Humana, T., Correa, P.G. Comparative analysis of cost, emissions and fuel consumption of diesel, natural gas, electric and hydrogen urban buses. Energy Conversion and Management, 257 (2022) article n. 115412.

[3] Rivarolo, M., Freda, A., Traverso, A., Test campaign and application of a small-scale ducted wind turbine with analysis of yaw angle influence. Applied Energy, 279 (2020) 115850_1-9.

[4] Giourka, P., Apostolopoulos, V., Angelakoglou, K., Kourtzanidis, K., Nikolopoulos, N., Sougkakis, V., Fuligni, F., Barberis, S., Verbeek, K., Costa, J.M., Formiga, J., The nexus between market needs and value attributes of smart city solutions towards energy transition. An empirical evidence of two european union (EU) smart cities, evora and alkmaar. Smart Cities, 3 (2020) 604-641.

[5] Ferrari, M.L., Traverso, A., Pascenti, M., Massardo, A.F., Plant management tools tested with a small-scale distributed generation laboratory. Energy Conversion and Management, 78 (2014) 105–113.

[6] Senyel Kurkcuoglu, M.A., Analysis of the energy justice in natural gas distribution with Multiscale Geographically Weighted Regression (MGWR). Energy Reports, 9 (2023) 325-337.

[7] Cassetti, G., Boitier, B., Elia, A., Le Mouël, P., Gargiulo, M., Zagamé, P., Nikas, A., Koasidis, K., Doukas, H., Chiodi, A., The interplay among COVID-19 economic recovery, behavioural changes, and the European Green Deal: An energy-economic modelling perspective. Energy, 263 (2023) 125798.

[8] Amirthan, T., Perera, M.S.A., The role of storage systems in hydrogen economy: A review. Journal of Natural Gas Science and Engineering, 108 (2022) 104843.

[9] Gadducci, E., Lamberti, T., Bellotti, D., Magistri, L., Massardo, A.F., BoP incidence on a 240 kW PEMFC system in a ship-like environment, employing a dedicated fuel cell stack model. International Journal of Hydrogen Energy, 46 (2021) 24503-24317.

[10] Bellotti, D., Rivarolo, M., Magistri, L., A comparative techno-economic and sensitivity analysis of Power-to-X processes from different energy sources. Energy Conversion and Management, 260 (2022) 115565_1-15.
[11] Reboli, T., Ferrando, M., Traverso, A., Chiu, J.N.W., Thermal energy storage based on cold phase change materials: Charge phase assessment. Applied Thermal Engineering, 217 (2022) 119177_1-12.
[12] Zhou, J., Xu, Z., Optimal sizing design and integrated cost-benefit assessment of stand-alone microgrid system with different energy storage employing chameleon swarm algorithm: A rural case in Northeast China. Renewable Energy, 202 (2023) 1110-1137.
[13] Akpinar, K.N., Gundogdu, B., Ozgonenel, O., Gezegin, C., An intelligent power management controller for grid-connected battery energy storage systems for frequency response service: A battery cycle life approach. Electric Power Systems Research, 216 (2023) 109040.
[14] Barberis, S., Rivarolo, M., Bellotti, D., Magistri, L., Heat pump integration in a real poly-generative energy district: A techno-economic analysis. Energy Conversion and Management: X, 15 (2022) 100238_1-10.
[15] Terlouw, T., AlSkaif, T., Bauer, C., Mazzotti, M., McKenna, R., Designing residential energy systems considering prospective costs and life cycle GHG emissions. Applied Energy, 331 (2023) 120362.
[16] Bouakkaz, A., Mena, A.J.G., Haddad, S., Ferrari, M.L., Efficient energy scheduling considering cost reduction and energy saving in hybrid energy system with energy storage. Journal of Energy Storage, 33 (2021) 101887_1-13.
[17] Rossi, I., Banta, L., Cuneo, A., Ferrari, M.L., Traverso, A.N., Traverso, A., Real-time management solutions for a smart polygeneration microgrid, Energy Conversion and Management, 112 (2016) 11-20.
[18] Reboli, T., Ferrando, M., Mantelli, L., Gini, L., Source, A., Garcia, J., Guedez, R., Gas Turbine Combined Cycle Range Enhancer – Part 1: Cyber-Physical Setup, ASME Paper GT2022-82494, ASME Turbo Expo 2022, Rotterdam, The Netherlands (2022).
[19] https://www.robinson-h2020.eu/
[20] https://www.dime.unige.it/en/research/laboratories/innovative-energy-systems-ies-uo-hi-sea-idrogeno-fuel-cells
[21] Traverso, A., TRANSEO code for the dynamic performance simulation of micro gas turbine cycles. ASME Paper GT2005-68101, ASME Turbo Expo, Reno, Nevada (USA).
[22] Bazmi, A.A., Zahedi, G., Sustainable energy systems: role of optimization modeling techniques in power generation and supply – A review. Renewable and Sustainable Energy Review, 15 (2011) 3480–500.
[23] Wang, H., Abdollahi, E., Lahdelma, R., Jiao, W., Zhou, Z., Modelling and optimization of the smart hybrid renewable energy for communities (SHREC). Renewable Energy, 84 (2015)114–123.
[24] Sayedin, F., Maroufmashat, A., Sattari, S., Elkamel, A., Fowler, M., Optimization of photovoltaic electrolyzer hybrid systems taking into account the effect of climate conditions. Energy Conversion and Management, 118 (2016) 438–149.
[25] Wang, X., Palazoglu, A., El-Farra, N.H., Operational optimization and demand response of hybrid renewable energy systems. Applied Energy, 143 (2015) 324–135.
[26] https://cordis.europa.eu/programme/id/H2020-EC
[27] Jaatinen-Värri, A., Nerg, J., Uusitalo, A., Ghalamchi, B., Uzhegov, N., Smirnov, A., Malkamäki, M., Design of a 400 kW Gas Turbine Prototype. ASME Turbo Expo 2016, Paper No: GT2016-56444 (2016).
[28] Rivarolo, M., Rattazzi, D., Magistri, L., Best operative strategy for energy management of a cruise ship employing different distributed generation technologies. International Journal of Hydrogen Energy, 43 (2018) 23500-23510.
[29] Audet, C., Dennis J.E., Analysis of Generalized Pattern Searches. SIAM Journal on Optimization, 13 (2003) 889–903.
[30] Lewis, R.M., Shepherd, A., Torczon, V., Implementing generating set search methods for linearly constrained minimization. SIAM Journal on Scientific Computing, 29 (2007) 2507–2530.
[31] Wang, L., Model Predictive Control System Design and Implementation Using MATLAB®, Springer London, UK (2009).
[32] Wang, L., Young, P.C., An improved structure for model predictive control using non-minimal state space realization. Journal of Process Control, 16 (2006) 355-371.
[33] Reboli, T., Ferrando, M., Mantelli, L., Gini, L., Sorce, A., Garcia, J., Guedez, R., Gas turbine combined cycle range enhancer – part 1: cyber-physical setup. ASME Turbo Expo 2022, ASME Paper GT2022-82494, Rotterdam, The Netherlands (2022).
[34] Cuneo, A., Greco, A., Rivarolo, M., Massardo, A.F., Design optimization of smart poly generation grids through a model based approach. Proceedings of ECOS 2014, June 15-19, Turku, Finland.
[35] Maamouri, R., Guilbert, D., Zasadzinski, M., Rafaralahy H., Proton exchange membrane water electrolysis: Modeling for hydrogen flow rate control. International Journal of Hydrogen Energy, 46 (2021) 7676-7700.
[36] Mantelli, L., Ferrari, M.L., Traverso A., Dynamics and control of a turbocharged solid oxide fuel cell system. Applied Thermal Engineering, 191 (2021) 116862_1-14.
[37] Ghigliazza, F., Traverso, A., Massardo, A.F., Wingate, J., Ferrari, M.L., Generic Real-Time Modeling of Solid Oxide Fuel Cell Hybrid Systems. Journal of Fuel Cell Science and Technology, Vol. 6 (2009) 021312_1-7.
[38] Ferrari, M.L., Traverso, A., Pascenti, M., Massardo, A.F., Early Syart-Up of Solid Oxide Fuel Cells Hubrid Systems with Ejector Cathodic Recirculation: Experimental Results and Model Verification. Proc. IMechE, Part A, Power and Energy, 221 (2007) 627-635.
[39] Carrero, M.M., De Paepe, W., Bram, S., Musin, F., Parente, A., Contino, F., Humidified micro gas turbines for domestic users: An economic and primary energy savings analysis. Energy, 117 (2016) 429-438.

[40] https://www.clean-hydrogen.europa.eu/system/files/2014-09/study%2520electrolyser_0-Logos_0_0.pdf